FACET ENGINEERING CHARGE SELECTIVITY IN OVERALL

WATER SPLITTING SYSTEMS

by

KADEN WHEELER

A THESIS

Presented to the Department of Chemistry and Biochemistry
and the Robert D. Clark Honors College
in partial fulfillment of the requirements for the degree of
Bachelor of Science

May 2023

An Abstract of the Thesis of

Kaden Wheeler for the degree of Bachelor of Science
in the Department of Chemistry and Biochemistry to be taken June 2023

Title: Facet Engineering Charge Selectivity in Overall Water Splitting Systems

Approved: _Shannon Boettcher, Ph.D._
Primary Thesis Advisor

In the midst of a growing energy crisis, green energy is a central point of conversation. Green energy can be efficiently created in electrochemical devices via water electrolysis. Semiconductors can be used in electrochemical devices, specifically photoelectrochemical devices, that absorb light and convert the absorbed energy to split water. Strontium titanate (STO) nanoparticles is a large band gap semiconductor that has been shown to be highly efficient at absorbing UV light and using UV light to split water in the presence of a metal catalyst. While this is accepted for STO, this phenomenon is not understood fundamentally. Using electrochemical analytical techniques, metal catalyzed STO was investigated in order to begin to understand this phenomenon. While the results of macroscopic analysis of cobalt co-catalyzed STO was inconclusive, the pH dependence of STO's varying crystal facets hinted towards charge selectivity at the surface.

Acknowledgements

I would like to think Dr. Shannon Boettcher and Aaron Kaufmann for all the help throughout this process.

Table of Contents

List of Figures

# Introduction

The global energy crisis is one of the most prevalent problems in the world that is on many people's minds. Photoelectrochemistry provides a simple system for green energy. Similar to how plants use light to make sugars for energy, photoelectrochemical processes can use light to make gaseous hydrogen for energy from water e.g., water electrolysis. Water, one of the most abundant resources on Earth, can be converted into a small, energy dense molecule, hydrogen. Semiconductors are an important part in photoelectrochemical (PEC) devices that can be used to drive water electrolysis. Yet, the most efficient PEC devices only split water at efficiencies slightly higher than 10%, where the ideal devices approach efficiencies of up to 15%.[1] There is much more to learn about these devices to further optimize them for water electrolysis.

Water electrolysis (Scheme 1) is the splitting of water to form hydrogen and oxygen. This is done via two processes, an oxidation of water and a reduction of protons. Notice the presence of h^+ (holes) and e^- (electrons). Electrons are typically known, but holes may not be. A hole is an empty electronic state that would be otherwise filled with an electron, like an air bubble in a glass of water. In semiconductors, when an electron is excited, it leaves behind an empty space, the hole (an electron-hole pair). The resulting hydrogen that is created from this process can be collected, and later split to produce energy, thus creating a process for sustainable energy production.
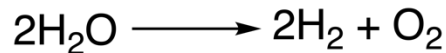
Oxidation:

$$2H_2O + 4h^+ \longrightarrow 4H^+ + O_2$$

Reduction:

$$4H^+ + 4e^- \longrightarrow 2H_2$$

Overall:

$$2H_2O \longrightarrow 2H_2 + O_2$$
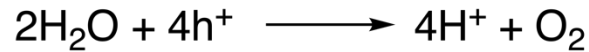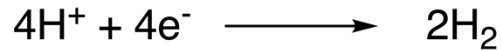
Scheme 1: Half-Reactions for Water Electrolysis

Water splitting half reactions, oxidation and reduction, and the combination of the two to yield the net reaction.

This experiment will investigate a wide bandgap semiconductor, strontium titanate (STO), that has been shown to split water efficiently when illuminated with ultraviolet light. This was shown on nanoparticles in the presence of a catalyst. Outside of the UV range however, STO splits water very poorly, because light is no longer absorbed.[2] The mechanisms for which STO splits water within the UV range, with a catalyst, are then important to understand to further optimize PEC devices.

STO nanoparticles has a few important features that allow for these high efficiencies. The two crystal facets, <100> and <110> (Figure 1), are adjacent to each other on the nanoparticles which allows for a much shorter distance for electrons, and holes, to travel before they can possibly recombine i.e., a large minority carrier diffusion length. This minority carrier diffusion length is larger than the nanoparticle. Finally, it is believed that STO crystal facets are charge selective.[2]
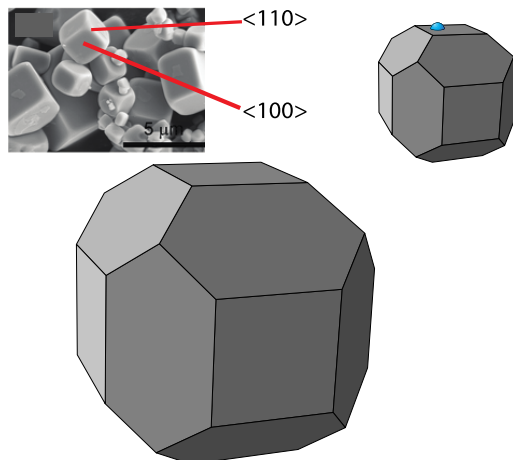
Figure 1: STO Nanoparticle

Drawings of STO nanoparticles. The larger one shows uncatalyzed STO and labels which crystal facet is which geometry, while the smaller one shows small, metal catalysts bound to the surface of the STO nanoparticle. Assumed charge selectivity to the surface is depicted. The top left is an image of the nanoparticles with the crystal facets labeled.[3]

This selective contact may be due to surface dipoles. The arrangement of molecules varies at different surface terminations of STO (Figure 2). This variation likely creates differing surface dipoles which can lead to this charge selectivity, as the exposure of different atoms creates a variation in the distribution of charge across the surface. Electrons and holes will then favor one crystal facet instead of another based on the charge distribution of these surfaces. The <100> crystal facet is thought to be selective to electrons, while the <110> crystal facet is thought to be selective to holes.[2]

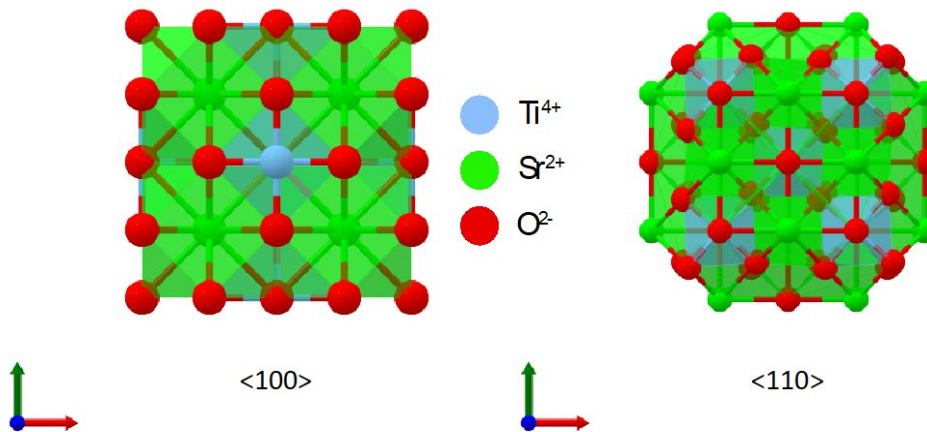Figure 2: Side-by-side comparison of STO <100> and STO <110> crystal facets.

The molecular geometry of STO's different crystal facets. The different arrangement of molecules may cause the observations seen on the nanoparticle scale.[4]

The nanoparticle case is where most of these phenomena have been observed, but charge selectivity at specific crystal facets does not change when moving from the nanoparticle scale to the single crystal scale. Electrochemical analysis on the two scales also provides similar results.[5,6] Due to these similarities, this phenomenon can be studied on both the nanoparticle and single crystal scale, and the results will be applicable to both scales.

In order to study the observed charge selectivity, the <100> and <110> crystal facets will be compared in the presence of cobalt, deposited in two different conditions: reductive and oxidative. Due to the selectivity of electrons and holes, cobalt may selectively deposit to one crystal facet instead of the other in these varying conditions. However, cobalt is observed to selectively deposit onto the <110> crystal facet,[2] thus depositing cobalt in reducing conditions may be inconclusive.

This work will also investigate the effect of pH on the open circuit voltage (V_{OC}) of STO <100> and <110>, and with platinum deposited onto the <100> crystal face. The two crystal

9

facets will likely act differently in the presence of metal catalysts across varying pHs which may help point to charge selectivity at these crystal facets.

Photoelectrochemistry:

Electrochemistry is the subfield of chemistry that cares about the flow of electrons, or current, and photoelectrochemistry is electrochemistry with the addition of light. Electrochemically analyzing systems gives insight into specifics of a chemical reaction: the energy it takes to start the reaction, the energy transfer, the type of reaction, etc. The specific ways electrochemical techniques are applied in this experiment are discussed in the "Methods" section.

Data and Analysis

Uncatalyzed STO

In order to understand the mechanism of catalyzed STO, uncatalyzed STO must be understood. Water splitting is a redox reaction (Scheme 1) and because of this the reduction and oxidation of water correspond to positive and negative current in the cyclic voltammograms (CVs). A CV is taken by applying a known potential through an electrochemical cell, and the resulting current response of the system is measured. In pure water, identifying the chemical processes in a CV is straightforward. Positive current typically corresponds to the oxidation of water to form oxygen gas, or the oxygen evolution reaction (OER). Negative current corresponds to the reduction of water to form hydrogen gas, or the hydrogen evolution reaction (HER). These reactions are seen above in Scheme 1. Figure 3 shows CVs for both STO crystal facets. The y-axis is current density ($\mu A/cm^2$), showing the current response of STO to at the applied potential. The x-axis is the applied potential (V), referenced off of RHE (reversible hydrogen electrode). The shaded yellow region corresponds to the photocurrent that is seen when light from a xenon arc lamp is shone on the electrodes which has been normalized to the surface area of the electrode. When 1 sun intensity (100 mW/cm^2) is shone on the electrode, slightly less than 600 $\mu A/cm^2$ of current density is expected on STO.
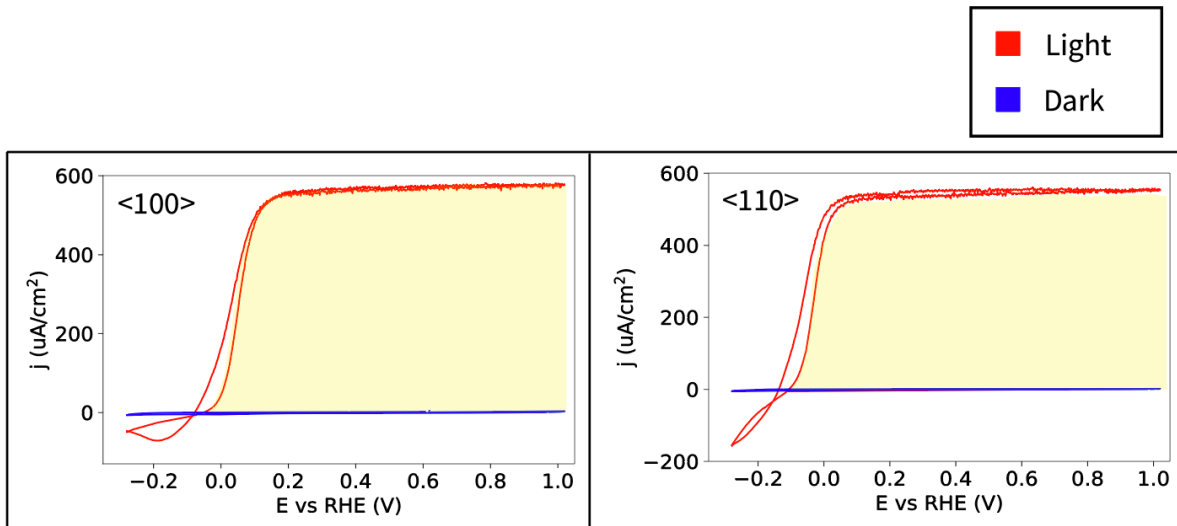
Figure 3: Uncatalyzed STO CVs

Cyclic voltammograms of STO <100> (left) and <110> (right) shown in both light (red) and dark (blue). The shaded yellow between the curves shows the photocurrent upon illumination.

A way to characterize and compare the results of STO in differing conditions, such as catalyzed and uncatalyzed, is by comparing the open circuit voltage (V_{OC}) of the semiconductor in light conditions. This is measured by taking the voltage where the light curve of our CV crosses 0 $\mu A/cm^2$ and reference this value off of the oxygen evolution reaction, or 1.23 V vs RHE. The V_{OC} is a good indicator of the performance of our photoelectrode, giving a good baseline for comparison, and a way to measure the photovoltage of the electrode. For the uncatalyzed results, the <100> has a V_{OC} of -1.298 ± 0.003 V vs OER, while the <110> has a V_{OC} of -1.347 ± 0.004 V vs OER. These results are then a baseline to see how the presence of cobalt on the different crystal facets affects the performance of STOs different crystal facets; the more negative the photovoltage, the electrode is better performing.

Cobalt Catalyzed STO

These STO electrodes then had cobalt photodeposited in oxidative and reductive conditions as discussed in the methods (Figure 4). The oxidative results saw fairly large current, above 50 μA. Therefore, the total time needed to pass enough charge through the electrode was very short and a small amount of cobalt oxide was seen on the surface of these electrodes. However, in the reducing conditions, the amount of current passed was very close to 0 mA. One would assume that the amount of cobalt on these electrodes would be near 0; if no current is passed, no cobalt can be deposited. When inspecting the surface of the electrodes with a microscope, it becomes obvious that a lot of cobalt was deposited, more than in the oxidative case. This is likely because these electrodes were held at this potential for a much longer time, and there were two competing process that are not directly seen in these results. There is a reductive process that is due to being held at high, negative voltage, and an oxidative process due to the photocurrent. After inspecting these electrodes with a microscope to see if cobalt was successfully deposited, CVs were performed on these electrodes to compare results with the uncatalyzed counter parts.
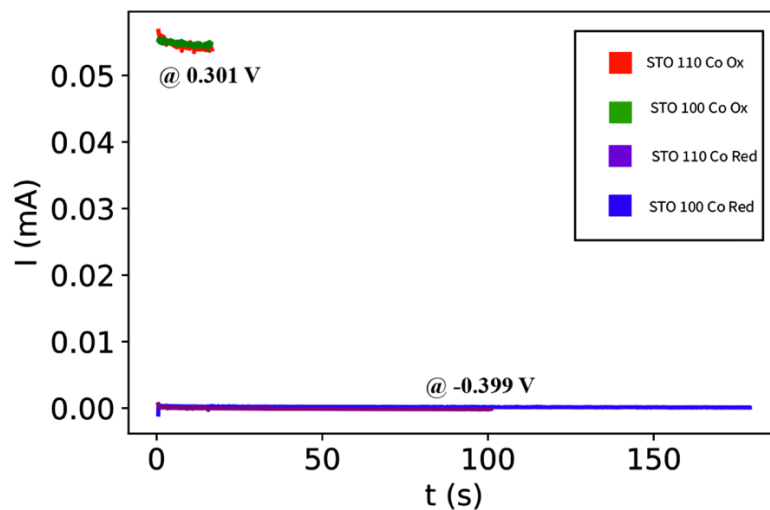
Figure 4: Photodeposition scans to deposit Co.

Current (mA) versus time (s) showing the photodeposition experiments on STO <100> and <110>. Co Red is for the electrodes that were deposited in reducing conditions. Co Ox is for the electrodes that were deposited in oxidative conditions. The corresponding applied voltage (referenced to HER) is shown by the results.

Results for the cobalt reduced onto STO (Figure 5) are similar to that of uncatalyzed at first glance. However, the photocurrent density on the <110> crystal facet with cobalt reduced to the surface increased. This is interesting because this electrode did not have as much cobalt reduced to the surface as its <100> counterpart. The amount of cobalt deposited then may scale with diminishing returns, i.e., there is some amount of cobalt that maximizes the amount of photocurrent produced, and any more or less scales the photocurrent differently. At this optimal amount of cobalt, there may be enough cobalt on the surface such that every electron-hole pair that is generated has a nearby cobalt nanoparticle that can collect electrons and drive water splitting. Less cobalt deposited may mean that electron-hole pairs are recombining before a cobalt nanoparticle can collect them to drive water splitting, and any more cobalt may be blocking too much light and thus less electron-hole pairs are generated.
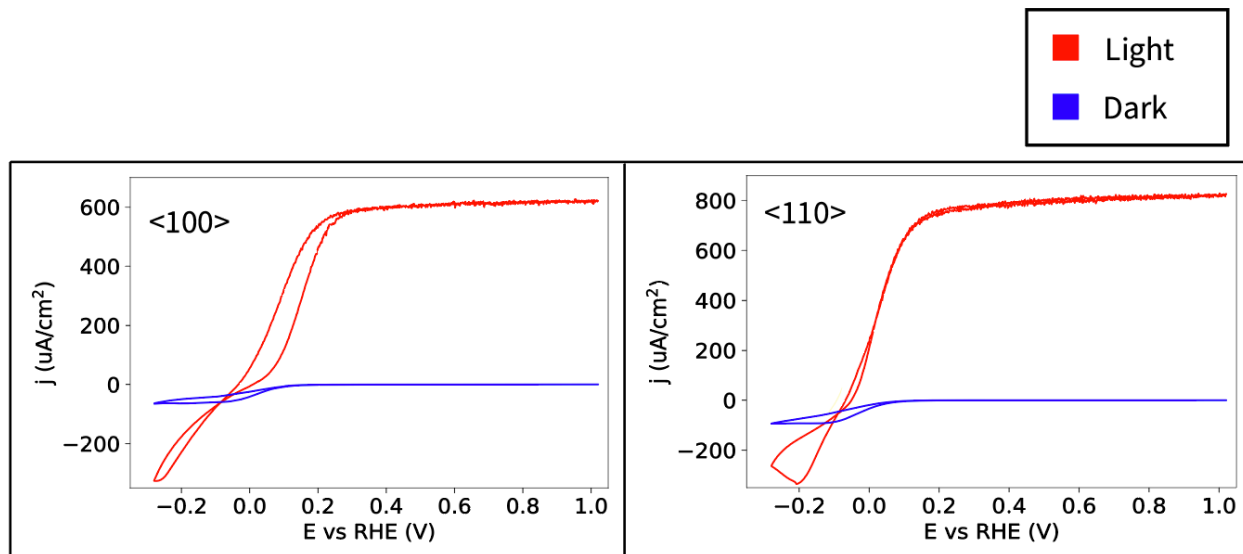
14

Figure 5: Cobalt Reductive CVs.

CVs of STO <100> and <110> with cobalt photodeposited on the surface in reducing conditions.

The V_{OC} for the <100> with cobalt reduced to the surface is -1.243 ± 0.008 V vs OER. The V_{OC} for the <110> is -1.293 ± 0.006 V vs OER. This decrease could be due to STO losing performance in the presence of Co reduced to the surface. Similar decreases in photovoltage were seen in both the <100> and <110> crystal facets, therefore this would only tell us that reducing cobalt to the surface of STO is a poor method of deposition. However, the more likely reason that a decrease in photovoltage for both crystal facets is seen is because there was a large amount of cobalt deposited to both crystals. With more of the crystal's surface covered, less light can be absorbed, and a decrease in photovoltage would be expected.

These results can then also be compared to the results of oxidative cobalt deposition (Figure 6). The amount of photocurrent for both the <100> and <110> in the presence of cobalt oxide are comparable to that of the uncatalyzed STO results. Neither of the crystal facets show performance that seems to deviate in the presence of cobalt oxide, so the photovoltages must be compared.
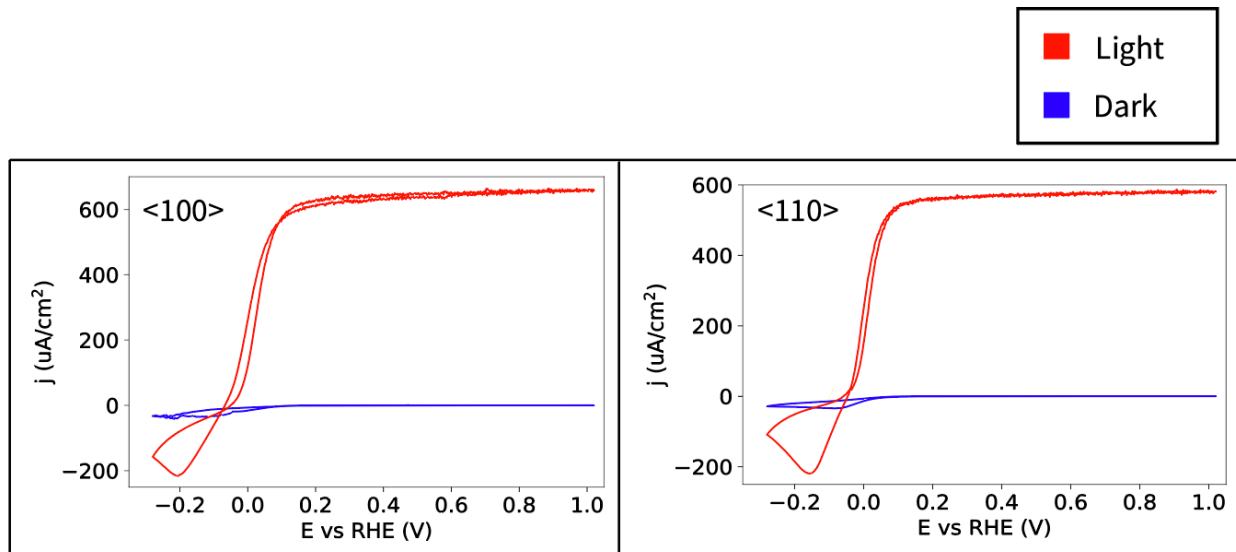
Figure 6: Cobalt Oxidative CVs.

CVs of STO <100> and <110> with cobalt photodeposited on the surface in oxidizing conditions.

STO <100> in the presence of CoOx has a photovoltage of -1.289 ± 0.002 V vs OER and STO <110> in the presence of CoOx has a photovoltage of -1.279 ± 0.008 V vs OER. Again, the data seems to point to the photoelectrode having worse performance in the presence of cobalt. However, this decrease in photovoltage is likely due to less light being absorbed from the cobalt blocking light. The difference between these results and the cobalt reduction results are very similar and neither the <100> or the <110> crystal facets observed any increase in performance due to the deposition of cobalt, nor a major decrease. Therefore, the cyclic voltammograms of these electrodes likely do not provide any results that strongly point to charge selectivity to specific crystal facets.

pH Experiments on STO

The next series of experiments compared the pH dependence of the <100> and <110> crystal facets open circuit voltage. These results were then also compared to the <100> with platinum nanoparticles deposited on the surface. First, for the <100> and <110> comparison

16

(Figure 8), STO <110> has a lower open circuit voltage across the entire pH scale. This means that STO <110> is a better photocatalyst for OER than the <100>, likely indicating that STO <110> has a higher selectivity to holes. Similarly, since the <100> has a higher open circuit voltage than the <110>, it is a worse OER photocatalyst, meaning it is less selective to holes (or more electron selective).
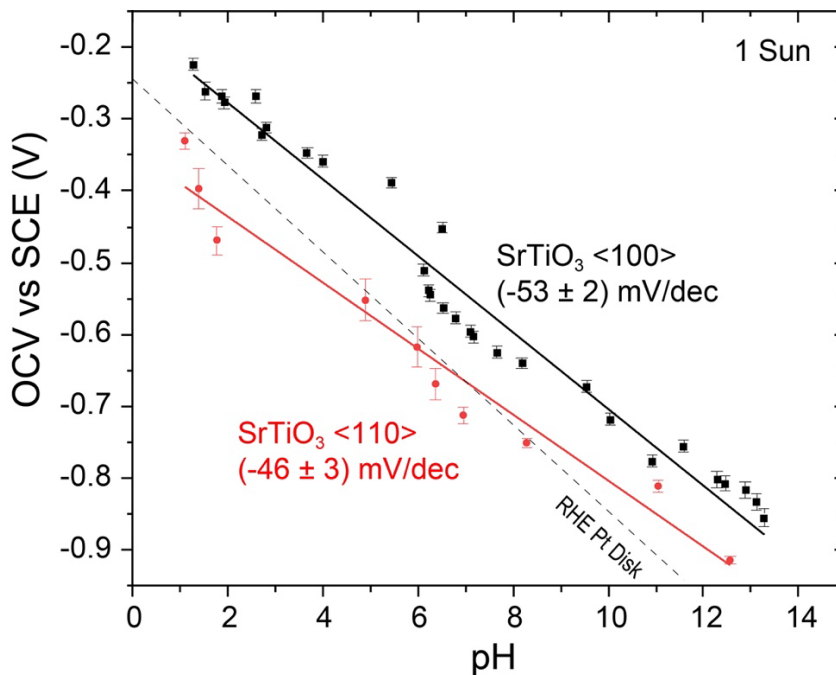

Figure 8: pH dependence of the V_{OC} of STO <100> and <110>

This plot shows the pH dependence of the open circuit voltage of STOs different crystal facets. A linear fit was performed and is plotted.

This study was then followed by depositing platinum nanoparticles onto the <100>
crystal facet and measuring its pH dependence (Figure 9). These results show that at lower pH's,
the <100> with platinum nanoparticles has a smaller open circuit voltage, yet at higher pH's, this
sample has a larger open circuit voltage. This is indicative that the selectivity of this electrode is
changing as the pH changes. At acidic pH's, the <100> with platinum nanoparticles is more
selective to electrons. As the pH increases, the sample becomes more selective to holes. This
may be due to the platinum being adaptive, thus changing the selectivity of the surface as the pH
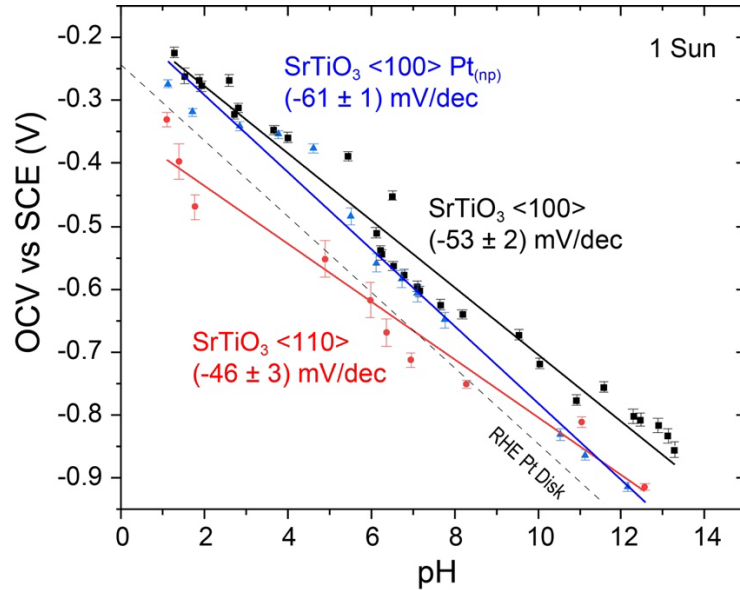changes.

Figure 9: pH dependence of the V_{OC} of STO <100> and <110>, and STO <100> with Pt
nanoparticles.

This plot shows the pH dependence of the open circuit voltage of STOs different crystal facets and
of STO <100> with Pt nanoparticles deposited onto the surface. A linear fit was performed and is
plotted.

Conclusion

While STO is a very suitable semiconductor for photoelectrochemical water splitting, the mechanisms in which it performs water splitting are still not completely understood. In order to begin understanding these mechanisms, it is important to know if STO has charge selective crystal facets or not. Charge selectivity has been previously hypothesized but has not been proven. This was investigated by comparing cyclic voltammograms of cobalt catalyzed STO to that of uncatalyzed STO, and by comparing the pH dependence of STO's open circuit voltage on the <100> and <110> crystal facets, as well as the <100> crystal facet with platinum nanoparticles deposited on the surface. While the cyclic voltammograms of STO in varying conditions did not directly point to any observed charge selectivity, the pH experiments pointed towards charge selectivity. Future experiments may investigate the pH dependence of STO <110> with either a platinum or cobalt co-catalyst. Similarly, CVs should be taken on STO in the presence of other co-catalysts such as rhodium or platinum.

Methods

Photodepositions

2 <100> and 2 <110> surface terminated STO crystals were fabricated into electrodes. One of each termination was placed in 0.01 M $CoCl_2$ and a chronoamperometry experiment was ran at -0.399 V vs SCE while illuminated with light of 1 sun intensity to photodeposit cobalt. This method reduces cobalt to the surface of STO. In order to compare this reduction process to the oxidation process, the same photodeposition experiment was repeated but the potentiostat was set to 0.301 V. This then oxidizes cobalt to the surface of the electrode.

Cyclic Voltammograms

Cyclic voltammograms use a potentiostat to shift an applied voltage across a range set by the researcher, and then the potentiostat measures the resulting current response.

After AFM experiments were ran, the electrodes were placed in 1 M semiconductor grade NaOH and cyclic voltammograms were ran in light, lit by a laser, and dark. The same experiments were run in 5 M NaOH, as well as illuminating the electrodes in 1 sun intensity light using a solar simulator. Each cyclic voltammogram was ran from -0.3 V to 1.0 V vs RHE (reversible hydrogen electrode). The reference electrode used in the measurements was a Mercury-Mercury Oxide reference electrode (Hg/HgO). The counter electrode was a platinum wire. The results for the STO cyclic voltammograms were standardized to RHE by first measuring RHE on a platinum disk working electrode.

pH Experiments

Cyclic voltammograms were ran on STO in 0.25 M HCl – 0.25 M H_3PO_4. A small scan window was chosen around the open circuit voltage. After each cyclic voltammogram, a

small amount of 1 M NaOH was pipetted into the solution, and another cyclic voltammogram

was taken. A pH probe was placed in solution in between cyclic voltammograms, and the pH of

the solution was recorded.

Citations

1. Segev, G.; Kibsgaard, J.; Hahn, C.; Xu, Z. J.; Cheng, W.-H. (Sophia); Deutsch, T. G.; Xiang, C.; Zhang, J. Z.; Hammarström, L.; Nocera, D. G.; Weber, A. Z.; Agbo, P.; Hisatomi, T.; Osterloh, F. E.; Domen, K.; Abdi, F. F.; Haussener, S.; Miller, D. J.; Ardo, S.; McIntyre, P. C.; Hannappel, T.; Hu, S.; Atwater, H.; Gregoire, J. M.; Ertem, M. Z.; Sharp, I. D.; Choi, K.-S.; Lee, J. S.; Ishitani, O.; Ager, J. W.; Prabhakar, R. R.; Bell, A. T.; Boettcher, S. W.; Vincent, K.; Takanabe, K.; Artero, V.; Napier, R.; Cuenya, B. R.; Koper, M. T. M.; Van De Krol, R.; Houle, F. The 2022 Solar Fuels Roadmap. *Journal of Physics D: Applied Physics* **2022**, *55* (32), 323003. https://doi.org/10.1088/1361-6463/ac6f97.
2. Takata, T.; Jiang, J.; Sakata, Y.; Nakabayashi, M.; Shibata, N.; Nandal, V.; Seki, K.; Hisatomi, T.; Domen, K. Photocatalytic Water Splitting with a Quantum Efficiency of Almost Unity. *Nature* **2020**, *581* (7809), 411–414. https://doi.org/10.1038/s41586-020-2278-9.
3. Ham, Y.; Hisatomi, T.; Goto, Y.; Moriya, Y.; Sakata, Y.; Yamakata, A.; Kubota, J.; Domen, K. Flux-Mediated Doping of SrTiO $_3$ Photocatalysts for Efficient Overall Water Splitting. *J. Mater. Chem. A* **2016**, *4* (8), 3027–3033. https://doi.org/10.1039/C5TA04843E.
4. "SrTiO3." *Materials Project*, materialsproject.org/materials/mp-5229#summary. Accessed 24 May 2023.
5. Kumar, G.; Chen, Z.-L.; Jena, S.; Huang, M. H. Facet-Dependent Optical and Electrical Properties of SrTiO3 Wafers. *J. Mater. Chem. C* **2023**, *11* (11), 3885–3888. https://doi.org/10.1039/D3TC00483J.
6. Hsieh, P.-L.; Madasu, M.; Hsiao, C.-H.; Peng, Y.-W.; Chen, L.-J.; Huang, M. H. Facet-Dependent and Adjacent Facet-Related Electrical Conductivity Properties of SrTiO3 Crystals. *J. Phys. Chem. C* **2021**, *125* (18), 10051–10056. https://doi.org/10.1021/acs.jpcc.1c01047.